



Method for rapid warning and activity concentration estimates in online water γ -spectrometry systems

Meng Wang¹ · Yi Gu^{1,2} · Mao-Lin Xiong¹ · Liang-Quan Ge^{1,2} · Qing-Xian Zhang^{1,2} · Guo-Qiang Zeng^{1,2} · Heng Lu¹ · Sheng-Liang Guo³

Received: 21 June 2023 / Revised: 15 September 2023 / Accepted: 22 September 2023 / Published online: 3 May 2024

© The Author(s), under exclusive licence to China Science Publishing & Media Ltd. (Science Press), Shanghai Institute of Applied Physics, the Chinese Academy of Sciences, Chinese Nuclear Society 2024

Abstract

Online γ -spectrometry systems for inland waters, most of which extract samples in situ and in real time, are able to produce reliable activity concentration measurements for waterborne radionuclides only when they are distributed relatively uniformly and enter into a steady-state diffusion regime in the measurement chamber. To protect residents' health and ensure the safety of the living environment, better timeliness is required for this measurement method. To address this issue, this study established a mathematical model of the online water γ -spectrometry system so that rapid warning and activity estimates can be obtained for water under non-steady-state (NSS) conditions. In addition, the detection efficiency of the detector for radionuclides during the NSS diffusion process was determined by applying the computational fluid dynamics technique in conjunction with Monte Carlo simulations. On this basis, a method was developed that allowed the online water γ -spectrometry system to provide rapid warning and activity concentration estimates for radionuclides in water. Subsequent analysis of the NSS-mode measurements of ^{40}K radioactive solutions with different activity concentrations determined the optimum warning threshold and measurement time for producing accurate activity concentration estimates for radionuclides. The experimental results show that the proposed NSS measurement method is able to give warning and yield accurate activity concentration estimates for radionuclides 55.42 and 69.42 min after the entry of a 10 Bq/L ^{40}K radioactive solution into the measurement chamber, respectively. These times are much shorter than the 90 min required by the conventional measurement method. Furthermore, the NSS measurement method allows the measurement system to give rapid (within approximately 15 min) warning when the activity concentrations of some radionuclides reach their respective limits stipulated in the Guidelines for Drinking-water Quality of the WHO, suggesting that this method considerably enhances the warning capacity of in situ online water γ -spectrometry systems.

Keywords Water radioactivity monitoring · Dynamic detection efficiency · Rapid warning · Activity estimation

This work was supported by the National Natural Science Foundation of China (No. 42127807), Natural Science Foundation of Sichuan Province of China (Project No. 2023NSFSC0008), Uranium Geology Program of China Nuclear Geology (No. 202205-6), and the Sichuan Science and Technology Program (No. 2021JDTD0018).

✉ Yi Gu
guyi10@cdut.edu.cn

¹ College of Nuclear Technology and Automation Engineering, Chengdu University of Technology, Chengdu 610059, China

² Applied Nuclear Technology in Geosciences Key Laboratory of Sichuan Province, (Chengdu University of Technology), Chengdu 610059, China

³ Chengdu New Ray Technology Co. Ltd, Chengdu 610052, China

1 Introduction

With the growing scale of nuclear energy and the extensive application of non-power nuclear technology, radioactive effluents discharged from nuclear facilities increase the risk of radioactive contamination of receiving waters. The radioactivity levels of these effluents have therefore become a focus of efforts to monitor the radiation environments near nuclear facilities [1–3]. The main radionuclides measured by water γ -spectrometry include natural radionuclides (e.g., the U, Th, and Ac series as well as ^{40}K) and artificial radionuclides (e.g., ^{58}Co , ^{60}Co , ^{131}I , ^{134}Cs , ^{137}Cs , and $^{110\text{m}}\text{Ag}$) [4–6]. Two methods, laboratory analysis of samples collected at regular intervals [7–11] and in situ water radioactivity

measurements [12, 13], are primarily employed to monitor radioactive effluents discharged from nuclear facilities. In situ water radioactivity measurement is a widely used method owing to its advantages over laboratory analysis, such as a short measurement period, relatively simple procedure, and real-time monitoring. Based on the measurement environment, online water γ -spectrometry systems can be categorized into marine and inland-water radioactivity measurement systems.

Online water γ -spectrometry systems for measuring marine radioactivity can be approximately classified into float-, cruise-, and pull-type systems. Float-type online water γ -spectrometry systems include the MARNET marine γ -radiation monitoring network developed by the German Federal Ministry of the Environment [14], the POSEIDON floating monitoring system developed by the Hellenic Center for Marine Research (HCMR) [15, 16], the Sentinel-type marine radioactivity monitoring instrument jointly developed by the Marine Environment Laboratory of the International Laboratory of Marine Radioactivity (IAEA-MEL) and the Radiological Protection Institute of Ireland [17], and the KATERINA marine radioactivity detection system developed by the HCMR [18]. Cruise-type systems include the underwater radiation spectral identification system developed by the United States Department of Energy's Remote Sensing Laboratory [19] and the REM-10 series underwater radiation control system developed by the Kurchatov Institute of the Russian Research Center [20, 21]. Pull-type systems include the dual-probe marine in situ γ -radiation monitoring system developed by the IAEA-MEL [22, 23] and the Radiometric Environment Survey and Quantification (RESQ) towed γ -ray spectrometer developed by the University of Tokyo [24]. Monitoring networks have been established for some online water γ -spectrometry systems to monitor radioactivity in key waters. Marine radioactivity measurement systems are generally unequipped with effective shielding materials owing to the restrictions imposed by the measurement conditions. The relatively high ambient radiation in the background requires a continuous measurement over more than 24 h to reach the lower detection limit of a marine radioactivity measurement system [8, 25, 26].

Inland water is susceptible to significant disturbances and contains a large amount of sediment. Consequently, online water-spectrometry systems developed specifically for inland waters mostly extract samples in situ and in real time [27–29], which are subsequently filtered and directed to a measurement chamber for radioactivity measurements. Waterborne radionuclides follow a non-steady-state (NSS) diffusion regime (i.e., a nonuniform distribution pattern) during the initial period after entering the measurement chamber. Because an online water-spectrometry system cannot accurately quantify radionuclides under NSS conditions, a wait time must be set to allow the radionuclides to

transition from the NSS to a steady-state (SS) diffusion pattern (i.e., a uniform distribution pattern), after which their activity concentrations can be accurately measured.

Conventional quantitative analysis methods quantify radionuclides based on the stable detection efficiencies for radionuclides in an SS diffusion pattern. Generally, the Monte Carlo simulation technique and validation measurements of standard radionuclide solutions are used to establish the detection efficiency curves for characteristic γ -rays at different energy levels as well as to calculate the minimum detectable activity concentration, based on which radionuclides in water are quantified [30–36]. However, for an online water γ -spectrometry system designed for inland waters that extracts samples in situ and in real time, the waiting time for the radionuclides in a water sample inside the measurement chamber to transition from an NSS to an SS distribution pattern directly increases the time required by the system to estimate the radionuclide activity concentrations in the water sample. This reduces the system timeliness in monitoring and giving warning of water radioactivity. Consequently, this study presents a method that enables online water-spectrometry systems designed for inland waters to provide rapid warning and activity estimates under NSS conditions, thus being able to protect the health of residents and ensure the safety of the living environment in areas near nuclear facilities.

2 Instruments and methods

2.1 Online water γ -spectrometry system

The online water γ -spectrometry system used in this study extracts samples in situ and in real time. Figure 1 shows the structure of this measurement system, which consists primarily of a CeBr₃ detector, measurement chamber (made of low-background lead and oxygen-free copper), multichannel analysis unit, data storage system, communication unit, continuous water sampling device, and pollution tank. The water sample is extracted from the monitored waters and directed into the measurement chamber at a rate of 0.12 L/s through the continuous sampling device equipped with a prefiltration function. Both the inlet and outlet tubes of the measurement chamber have a diameter of 20 mm. Under the actual measurement conditions, the water in the measurement chamber is in continuous flow, the monitored waters enter through the inlet tube at the top and exit through the outlet tube at the bottom, and the measurement chamber is filled with water during the measurement.

The measurement unit includes the CeBr₃ detector and measurement chamber. The CeBr₃ detector, which is composed of three CeBr₃ scintillators, each with dimensions of $\phi 45$ mm \times 50 mm as shown in Fig. S1(a) in the

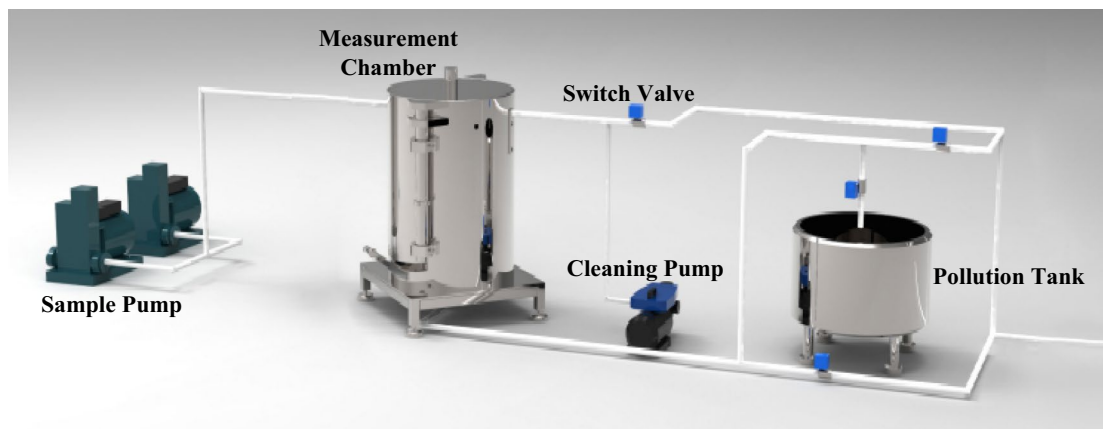


Fig. 1 (Color online) Main structure of the online water γ -spectrometry system

supplementary material, is used to improve the detection efficiency and responds to energy levels ranging from 30 to 3 MeV with a relative detection efficiency higher than 132% (@3 in NaI(Tl), 1.33 MeV, ^{60}Co). The measurement chamber has external dimensions of $\phi 740 \text{ mm} \times 720 \text{ mm}$ and internal dimensions of $\phi 496 \text{ mm} \times 596 \text{ mm}$. The measurement chamber has a supporting outer layer made of stainless steel and a 100-mm-thick internal layer made of lead. The inner side of the lead layer is covered with a 2-mm-thick oxygen-free copper layer and an ultrathin impermeable layer. The measurement chamber has a volume of 115 L. Figure S1(b) shows its detailed structure. The energy resolution of the measurement unit at the characteristic energy (662 keV) of ^{137}Cs is better than 4.5%. The lower detection limit for the 12 h measurement is 0.2 Bq/L for ^{137}Cs .

2.2 Non-steady-state (NSS) measurement model

When a water sample inside the measurement chamber follows the SS diffusion regime, the radionuclides contained in the sample are distributed uniformly inside the measurement chamber, with activity concentrations identical to those of the external source waters. Under these conditions, the detection efficiency of the measurement system for the characteristic γ -rays emitted from a certain radionuclide in the water is constant. In the SS measurement mode, the full energy peak (FEP) count rate for γ -rays can be described using the following equation:

$$n_{\text{SS}}(t) = C \cdot V \cdot \varepsilon_{\gamma} \cdot P_{\gamma}, \quad (1)$$

where $n_{\text{SS}}(t)$ is the FEP count rate for the characteristic γ -rays emitted from the radionuclide at time t , C is the activity concentration of the radionuclide in the measurement chamber (Bq/m^3), V is the volume of the measurement chamber (m^3), ε_{γ} is the detection efficiency for the

characteristic γ -rays emitted from the radionuclide in the measurement chamber, t is the measurement time (s), and P_{γ} is the emission probability of the characteristic γ -rays emitted from the radionuclide.

However, the distribution of the radionuclides inside the measurement chamber of an online water γ -spectrometry system in the NSS measurement mode changes dynamically. Consequently, the detection efficiency of the measurement system for the characteristic γ -rays emitted from a certain radionuclide in the water also changes dynamically. Therefore, when a measurement system is in NSS measurement mode, the FEP count rate for the characteristic γ -rays emitted from a radionuclide can be described using the following equation:

$$n_{\text{NSS}}(t) = A(t) \cdot \varepsilon(t) \cdot P_{\gamma}, \quad (2)$$

where $n_{\text{NSS}}(t)$ is the FEP count rate for the γ -rays at time t , $A(t)$ is the activity of the radionuclide inside the measurement chamber at time t (Bq), and $\varepsilon(t)$ is the detection efficiency for the characteristic γ -rays emitted from the radionuclide inside the measurement chamber at time t .

For an online water γ -spectrometry system in NSS measurement mode, because its detection efficiency for the characteristic γ -rays emitted from a certain radionuclide in the water is not constant, its FEP count for the γ -rays over a period of time from the starting moment to t , $N(t)$, can be obtained through an integration of Eq. (2):

$$N(t) = \int_0^t n(t) dt = \int_0^t A(t) \cdot \varepsilon(t) \cdot P_{\gamma} dt. \quad (3)$$

In the NSS measurement mode, the radionuclide in water that enters the measurement chamber does not completely remain inside the measurement chamber but is instead partially emitted from the measurement chamber with the exiting water. The calculation of the activity $A(t)$ of a

radionuclide in the measurement chamber requires the introduction of the proportion that remains in the measurement chamber, $f(t)$, into Eq. (3). $f(t)$ represents the ratio of the activity of the radionuclide inside the measurement chamber to the total activity of the cumulative amount of radionuclide that has entered the measurement chamber from the starting moment to t and is related to the structure of the measurement chamber and water flow rate. The activity of the amount of the radionuclide that remains inside the measurement chamber at time t can be calculated based on the flow rate of the radionuclide-containing water in the inlet tube of the measurement chamber of the online water γ -spectrometry system as well as the diameter of the inlet tube using the following equation:

$$A(t) = C \cdot v \cdot t \cdot f(t), \quad (4)$$

where C is the activity concentration of the radionuclide entering the measurement chamber (Bq/m^3), and v is the flow rate of water in the inlet tube of the measurement chamber (L/s).

Substituting Eqs. (4) into (3), the FEP count for the γ -rays at time t , $N(t)$, is obtained as follows:

$$N(t) = C \cdot v \cdot P_\gamma \cdot \int_0^t t \cdot f(t) \cdot \varepsilon(t) dt. \quad (5)$$

Two arbitrary time points, t_1 and t_2 , during the NSS measurement process were selected for the analysis and substituted into Eq. (5). The activity concentration of the radionuclide in the water flowing into the measurement chamber was then calculated using the following equation:

$$C = \frac{N(t_2) - N(t_1)}{P_\gamma \cdot v \cdot \int_{t_1}^{t_2} t \cdot \varepsilon(t) \cdot f(t) dt}. \quad (6)$$

The use of Eq. (6) to calculate the activity concentration of a radionuclide during the NSS measurement process requires obtaining the variables $f(t)$ and $\varepsilon(t)$ first.

3 Results

3.1 Residual percentage $f(t)$ of radionuclide

An analysis based on the diameter and water flow rate in the inlet tube of the measurement chamber revealed that the water that enters this chamber follows a turbulent flow regime. This presents challenges in determining the distribution patterns of the radionuclide at different time points and the variation in its concentration with time through mathematical description and direct measurements. Therefore, computational fluid dynamics (CFD) [37] was used to simulate the distribution pattern of radionuclides in

water after entry into the measurement chamber. Based on this, $f(t)$ in the NSS measurement mode was calculated. Figure 2 shows a schematic of the geometry of the input model constructed in the CFD simulation based on the actual dimensions of the measurement chamber of the online water γ -spectrometry system. The measurement chamber was composed of a cylinder with dimensions of $\phi 496 \text{ mm} \times 596 \text{ mm}$ and a hollow cylinder with dimensions of $\phi 140 \text{ mm} \times 363 \text{ mm}$. The hollow cylinder acted as a cavity to house the CeBr_3 detector. Both the inlet and outlet tubes of the measurement chamber had a diameter of 20 mm. The water flow rates in the two tubes were 0.12 L/s .

Figure 3a shows the analysis of the average radionuclide concentration across the measurement chamber during the diffusion process for the 100 Bq/L ^{40}K radioactive solution based on the domain probe module in the CFD simulation, and the average radionuclide concentration does not consider the effects of radionuclide decay. The radionuclide concentration in the water inside the measurement chamber becomes consistent with that in the source water only after a diffusion time of 90 min, suggesting that a wait time of at least 90 min is required to accurately quantify the radionuclide activity concentration in the water using the online water γ -spectrometry system coupled with the conventional measurement method.

Based on the analysis of the variation in the average radionuclide concentration inside the measurement chamber with the diffusion time, $f(t)$ can be calculated using the following equation for the online water γ -spectrometry system in the NSS measurement mode:

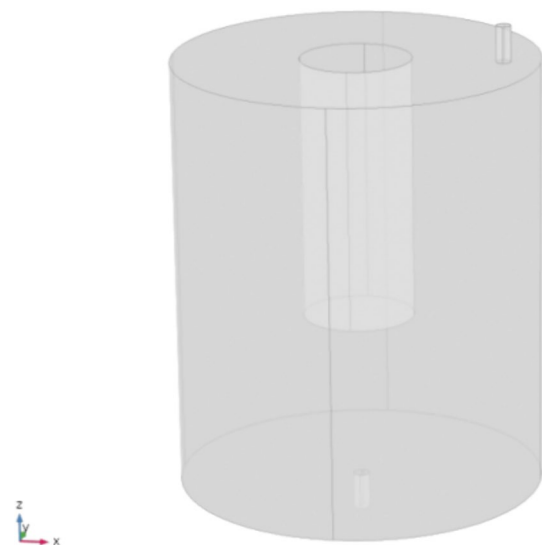


Fig. 2 Schematic of the geometry of the input model of the measurement chamber

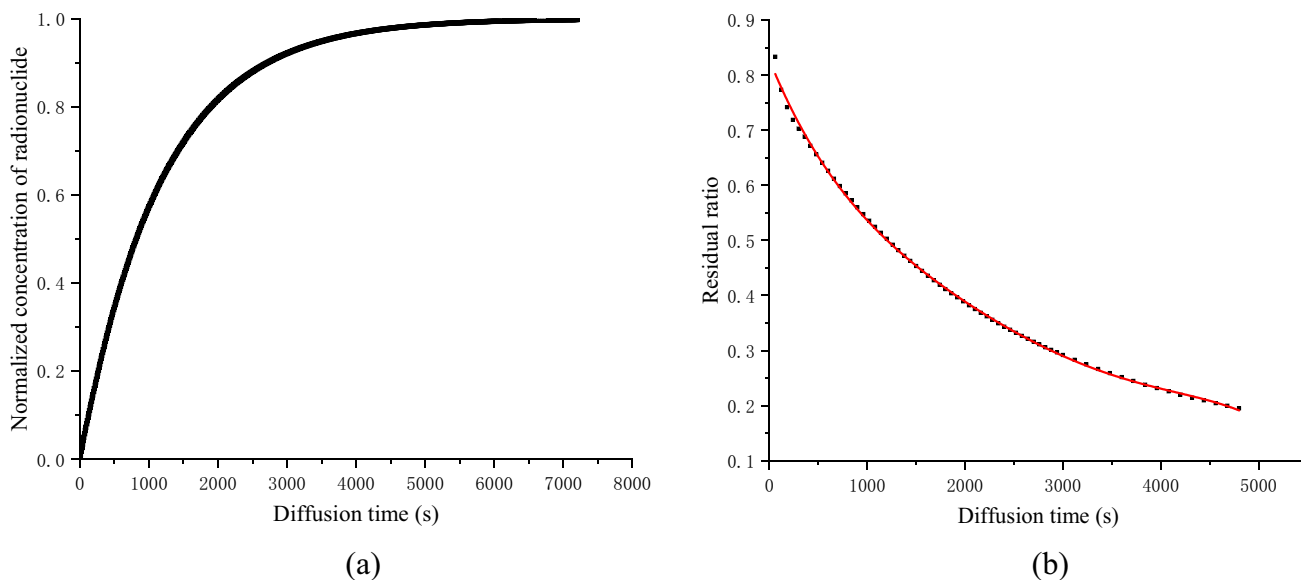


Fig. 3 Simulated diffusion of the radionuclides in the measurement chamber (curves depicting the variation in the **a** average concentration and **b** $f(t)$ of the radionuclides inside the measurement chamber with the diffusion time)

$$f(t) = \frac{C(t) \cdot V}{v \cdot t \cdot C}, \tag{7}$$

where v ($=0.12$ L/s) is the water flow rate in the inlet and outlet tubes during the dynamic measurement process, C ($=100$ Bq/L) is the radionuclide concentration in the source water outside the measurement chamber, $C(t)$ is the average radionuclide concentration inside the measurement chamber at time t (Bq/L), and V ($=0.115$ m³) is the volume of the measurement chamber.

Figure 3b shows the $f(t)$ values at different diffusion times, calculated using Eq. (7). An analysis of the calculation results provided a fitting equation for $f(t)$ and the diffusion time t ($R^2=0.998$), as shown in Eq. (8).

$$f(t) = 0.1343 + 0.6594 \times e^{\frac{-t}{2.0779 \times 10^3}} \tag{8}$$

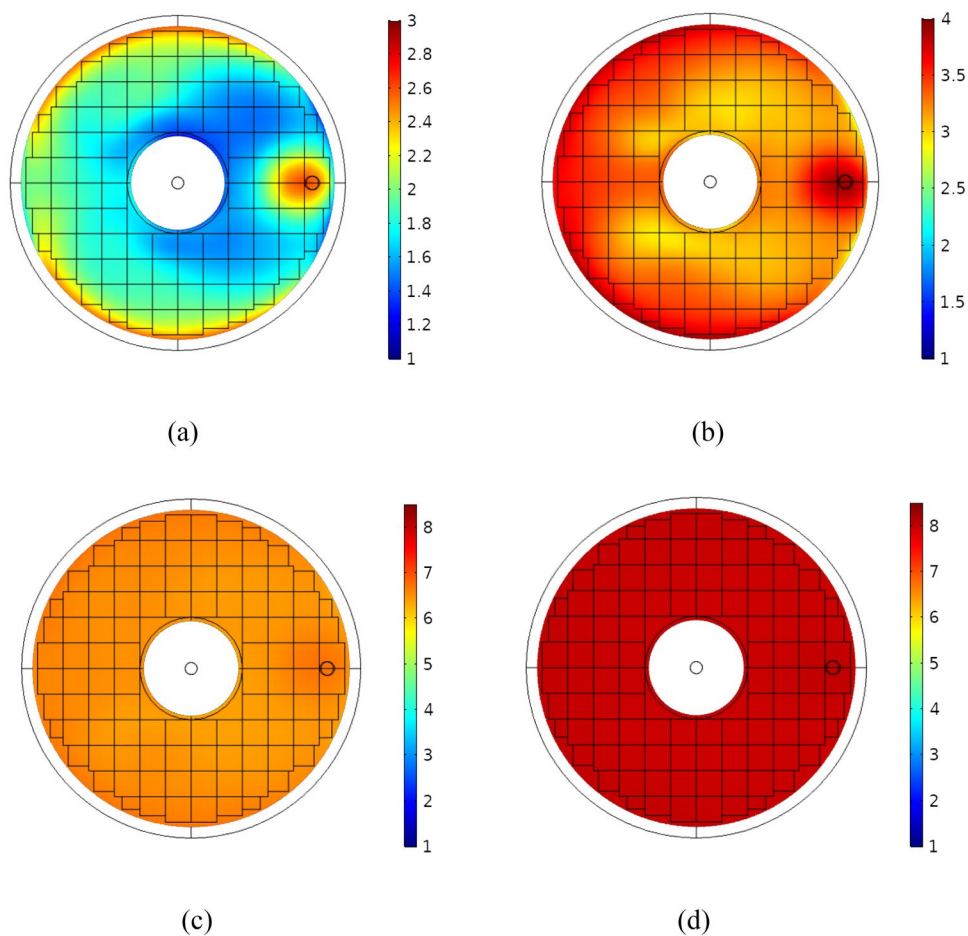
3.2 Monte Carlo simulations of the detection efficiency

To calculate the time-varying detection efficiency of the detector inside the measurement chamber for the characteristic γ -rays emitted from a radionuclide in the water in NSS measurement mode, a physical model of the source distribution corresponding to the radionuclide inside the measurement chamber was constructed based on the data obtained in Sect. 3.1 for the concentration distribution of the radionuclide during the NSS diffusion process. The concentration distribution of the radionuclides inside the measurement chamber during the NSS diffusion process cannot be

expressed as a function. Thus, the measurement chamber was divided into a finite number of water elements, which were then filled with the radionuclide concentrations in the water at different time points to simulate the detection efficiency of the measurement system under NSS conditions using the Monte Carlo technique in the open-source software Geant4. To ensure the accuracy of the data for the distribution of the radionuclide concentration inside the measurement chamber and considering the computational efficiency, the measurement chamber was divided into 17 layers, as shown in Fig. S2(a). Subsequently, as shown in Fig. S2(b), the water in each layer was divided into multiple cuboids/fan-shaped curved bodies. The entire measurement chamber was divided into 1864 water elements.

The radionuclide concentration of each water element in the measurement chamber was calculated using the water elements employed as domain probes in the CFD simulation. Figure 4 shows the distribution patterns of the radionuclide concentrations in each water element in the 7th layer of the measurement chamber 5, 10, 30, and 60 min after the radionuclide-containing water entered the measurement chamber. The radionuclide concentration in each water element continuously increased with radionuclide diffusion time. Similar radionuclide concentrations were reached in the different water elements in this layer 60 min after the radionuclide entered the measurement chamber. The mass of the radionuclides at different locations inside the measurement chamber was determined by multiplying the radionuclide concentrations obtained for all water elements by the volume of the corresponding area. The distribution patterns of the radionuclide concentration inside the measurement

Fig. 4 (Color online) Distribution patterns of the radionuclide concentration in each domain probe area in the 7th layer of the measurement chamber at diffusion times of **a** 5, **b** 10, **c** 30, and **d** 60 min



chamber at different diffusion times were then determined by normalizing the results obtained for all the water elements.

The geometry of the physical model constructed to calculate the detection efficiency through Monte Carlo simulation agreed completely with that of the measurement chamber. The radionuclide-containing water inside the measurement chamber was divided into the same number of water elements as those shown in Fig. S2 and sampled as the source term. The radionuclide concentration in each water element was set based on the corresponding normalized concentration determined by the CFD simulation. Figure S3 shows the physical structure of the model used to calculate the detection efficiency inside the measurement chamber through the simulation and partitioning of the model into water elements.

Monte Carlo numerical simulations yield curves depicting the variation in the detection efficiencies of the system for the characteristic γ -rays emitted from ^{40}K (1460.9 keV), ^{58}Co (810.77 keV), ^{60}Co (1332.51 keV), ^{131}I (364.49 keV), ^{134}Cs (604.72 keV), and ^{137}Cs (661.66 keV) inside the measurement chamber with the diffusion time, as shown in Fig. 5. The detection efficiency of the measurement system for radionuclides increased rapidly as the radionuclides continuously entered the measurement chamber during the initial stage.

When the diffusion time increased beyond 900 s, the distribution pattern of each radionuclide inside the measurement chamber remained almost unchanged, whereas the concentration of each radionuclide continuously increased. Under this condition, the detection efficiency of the measurement system for the characteristic γ -rays emitted from each radionuclide basically tends to stabilize.

The detection efficiencies of the measurement system for γ -rays at different energy levels in the NSS measurement mode obtained from Monte Carlo simulations reveal that they tend to level off 900 s after the entry of radionuclides into the measurement chamber. When the activity concentration of a radionuclide in the water is calculated, if the values of t_1 and t_2 in Eq. (6) are both set to be greater than 900 s, the detection efficiency $\varepsilon(t)$ can be considered as a constant, as presented in Table 1. Under these conditions, the cumulative count and activity concentration of the radionuclides in the NSS measurement mode can be calculated using the following equations:

$$N(t) = C \cdot v \cdot P_\gamma \cdot \varepsilon_\gamma \cdot \int_0^t t \cdot f(t) \cdot dt, \quad (9)$$

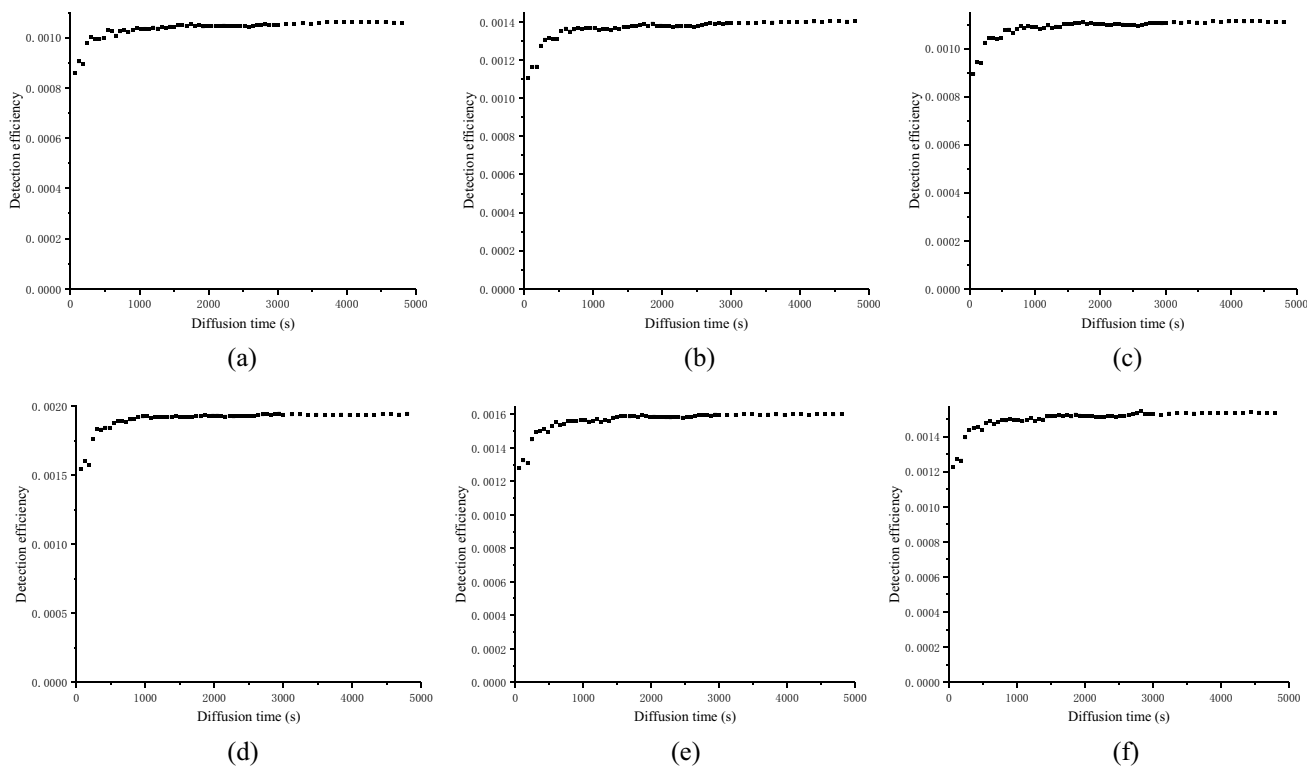


Fig. 5 Curves of the variation in the detection efficiency of the measurement system for the characteristic γ -rays emitted from **a** ^{40}K (1460.9 keV), **b** ^{58}Co (810.77 keV), **c** ^{60}Co (1332.51 keV), **d** ^{131}I

(364.49 keV), **e** ^{134}Cs (604.72 keV), and **f** ^{137}Cs (661.66 keV) with the diffusion time

Table 1 Detection efficiencies for γ -rays at different energy levels in non-steady-state (NSS) measurement mode

Radionuclide	γ -ray energy (keV)	Emission probability (%)	Detection efficiency ($\times 10^{-3}$)
^{40}K	1460.82	10.67	1.05
^{58}Co	810.71	99.45	1.39
^{60}Co	1332.51	99.98	1.10
^{131}I	364.49	81.24	1.93
^{134}Cs	604.72	97.60	1.59
^{137}Cs	661.66	84.62	1.53

$$C = \frac{N(t_2) - N(t_1)}{P_\gamma \cdot v \cdot \epsilon_\gamma \cdot \int_{t_1}^{t_2} t \cdot f(t) dt} \quad (10)$$

3.3 Experimental validation

The relative deviation between the cumulative count of the radionuclides given by the NSS measurement model and the cumulative count measurement directly reflects the measurement accuracy of the model for the radionuclide concentration. To prevent radioactive contamination of the

surrounding environment, ^{40}K , an easily accessible natural radionuclide, was used in the validation experiment. Different masses of KCl powder were dissolved in water to prepare ^{40}K radioactive solutions with six activity concentrations (5, 10, 20, 30, 40, and 60 Bq/L). Subsequently, the system was used to obtain the γ -spectrometry measurements for the ^{40}K radioactive solutions with different activity concentrations at different diffusion times in the NSS measurement mode, as shown in Fig. S4. Figure 6 shows the measured net FEP counts for ^{40}K radioactive solutions with different activity concentrations in the NSS measurement mode.

Analysis of the relative errors of the measured cumulative counts for the ^{40}K radioactive solutions with different activity concentrations from the theoretical values revealed a basic agreement between the measurements and theoretical calculations of the radionuclide in water. The high statistical fluctuation in the measured counts for each ^{40}K -containing radioactive solution in the first 20 min after its entry into the measurement chamber, owing to the relatively low activity concentration of ^{40}K in the chamber, led to a relatively significant relative error of the measurement from the theoretical calculation. A continuous increase in the activity concentration of ^{40}K in the measurement chamber decreased the relative error, which fell within $\pm 5\%$ after the first 20 min for each solution.

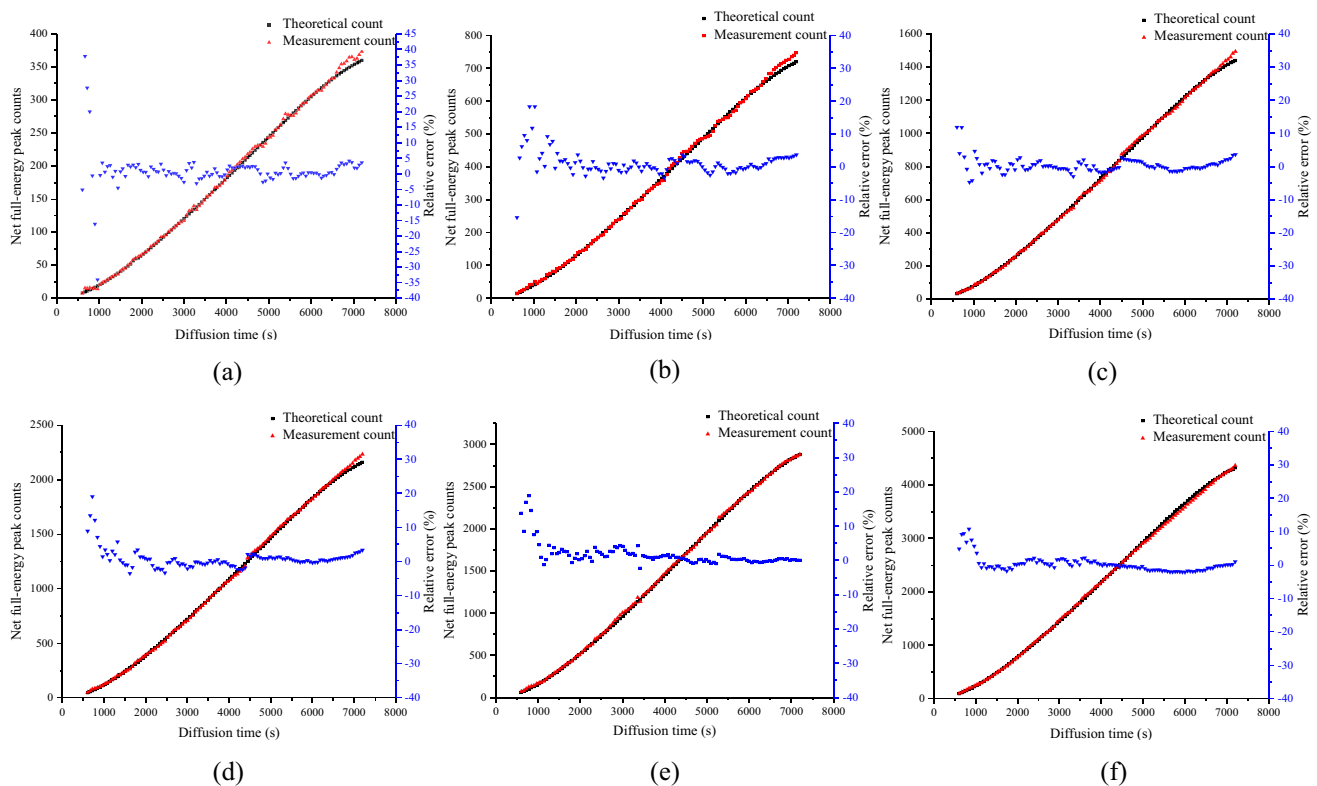


Fig. 6 (Color online) Measured net full energy peak (FEP) counts for the ^{40}K radioactive solutions with activity concentrations of **a** 5, **b** 10, **c** 20, **d** 30, **e** 40, and **f** 60 Bq/L

4 Discussion

4.1 Predictive analysis of radionuclides in water in the ideal measurement condition

To determine an optimum warning threshold and an optimum prediction time for the online water γ -spectrometry system in the NSS measurement mode, the NSS measurements of the 10 Bq/L ^{40}K radioactive solution were selected for analysis. An ideal measurement condition refers to a situation in which the specific entry time of the radionuclide-containing water into the measurement chamber is known. Under normal circumstances, radioactivity measurements at a confidence level of 0.95 are considered reliable. Based on eight γ -spectrometry measurements performed on the 10 Bq/L ^{40}K radioactive solution in the NSS diffusion mode, confidence levels and intervals were calculated for the net FEP counts for ^{40}K at 1460.9 keV at different diffusion times (as presented in Table S1 in the supplementary material). An average net FEP count of 143 ± 6.44 was determined for ^{40}K at 1460.9 keV 35 min after the beginning of the diffusion of the ^{40}K radioactive solution inside the measurement chamber, with a confidence level of greater than 0.95. The FEP background count at 1460.9 keV at this time was 214 ± 11.04 . The ratio of the cumulative FEP count to the

natural FEP background count was 1.67. The use of this ratio as a warning threshold for the water radioactivity measurement system is relatively reasonable.

When the NSS measurement model in Eq. (10) is used to estimate the radionuclide activity concentration in water, the time at which the warning threshold of the measurement system is reached can be selected as t_1 . Then, Eq. (10) can be used to calculate the radionuclide activity concentrations at different time intervals Δt between t_1 and t_2 (as listed in Table 2), and the uncertainty of the activity concentration estimate is the synthetic uncertainty, which is mainly contributed by the statistical fluctuation of the cumulative

Table 2 Activity concentration estimates for ^{40}K in the 10 Bq/L ^{40}K radioactive solution at different time intervals in the ideal measurement condition

Time interval Δt (min)	Activity concentration for ^{40}K (Bq/L)	Relative error (%)
1	5.71 ± 1.94	-42.90
5	7.65 ± 1.61	-23.50
10	9.33 ± 1.21	-6.70
15	9.50 ± 0.79	-5.00
20	9.83 ± 0.74	-1.70
30	9.86 ± 0.59	-1.40

FEP count. The calculation results in Table 2 reveal that at $\Delta t > 15$ min, the relative deviation of the radionuclide activity concentration in the water yielded by the NSS measurement model from the true value is less than 5%, suggesting that this model is effective at giving relative accurate estimates for radionuclide activity concentrations in water. Therefore, producing an accurate estimate of the radionuclide activity concentration in water requires measurements for an additional period of 15 min after the warning threshold of the measurement system is reached.

The time at which the warning threshold of the measurement system was reached varied with the activity concentration of ^{40}K in the ^{40}K radioactive solution. In addition, the use of the NSS measurement model to calculate the radionuclide activity concentration in water requires the determination of the diffusion time of the radionuclide when the warning threshold of the measurement system is reached, t_1 , and an interval of 15 min between t_1 and t_2 . Based on Eq. (9), the following equation is obtained:

$$t_2 = t_1 + 900, \tag{11}$$

$$\frac{N(t_2)}{N(t_1)} = \frac{\int_0^{t_2} t \cdot f(t) dt}{\int_0^{t_1} t \cdot f(t) \cdot dt}. \tag{12}$$

Analysis of the measurements determined the net FEP counts for ^{40}K at 1460.9 keV at t_1 and t_2 ($N(t_1)$ and $N(t_2)$, respectively), as well as their ratio k . Substituting Eqs. (8) and (11) into Eq. (12) gives the following higher-order equation with respect to t_1 :

$$D \cdot t_1^2 + E \cdot t_1 + F \cdot t_1 \cdot e^{-\frac{t_1}{\sigma}} + H \cdot e^{-\frac{t_1}{\sigma}} + I = 0 \tag{13}$$

Table 3 summarizes the values of coefficients D , E , F , G , H , and I in Eq. (13)

In summary, the following procedure can be used to calculate the radionuclide activity concentration in radioactively contaminated water. First, the ratio of the net FEP count for the characteristic γ -rays emitted from the radionuclide at the time when the preset warning threshold of the measurement system is reached to that at 15 min after reaching the warning threshold, k , is calculated. Subsequently,

Table 3 Values of the coefficients in Eq. (13)

Coefficients	Values
D	$6.7135 \times 10^{-2} \times (1 - k)$
E	1.2084×10^2
F	$8.8851 \times 10^2 - 1.3701 \times 10^3 \times k$
G	2.0779×10^3
H	7.9970×10^5
I	5.4379×10^4

substituting k into Eq. (13) determines the diffusion time of the radionuclide inside the measurement chamber when the warning threshold of the measurement system is reached, t_1 . Finally, substituting t_1 and t_2 into the NSS measurement model in Eq. (10) provides an activity concentration estimate for the radionuclide in the monitored water.

4.2 Predictive analysis of radionuclides in water in actual measurement conditions

In actual measurement conditions, to eliminate the impact of statistical fluctuations on measurements, the ratio of the cumulative FEP count for the characteristic γ -rays emitted from the radionuclide of interest in the water to the corresponding natural background count within a fixed time interval T is used to determine whether the warning threshold of the online water γ -spectrometry system for the radionuclide activity concentration is reached. In this study, a 10 Bq/L ^{40}K radioactive solution was selected for the measurement. Figure 7 shows the variation in the FEP count rate given by the online water γ -spectrometry system in NSS measurement mode for ^{40}K at 1460.9 keV with the measurement time. When the NSS measurement model is used to estimate the radionuclide activity concentration in water, accurately determining whether the measurement reaches the warning threshold requires the selection of a suitable time interval T to facilitate the acquisition of reliable measurement data.

As shown in Fig. 7, the measurement system must perform continuous measurements of the monitored water under actual measurement conditions. The use of the NSS measurement model to estimate the radionuclide activity concentration in water assumes that the radionuclide enters the measurement chamber at time $t = 0$ and that the warning threshold of the measurement system is reached at

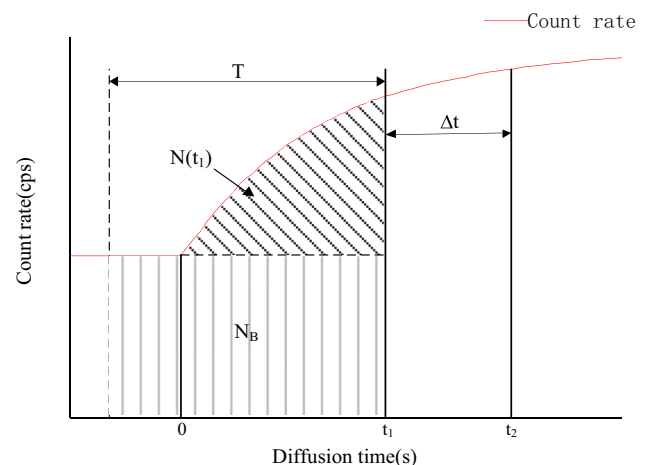


Fig. 7 Variation in the FEP count for ^{40}K at 1460.9 keV with the measurement time

time t_1 . The following can be obtained based on the warning threshold selected for ideal measurement conditions.

$$\frac{N(t_1) + N_B}{N_B} = 1.67, \tag{14}$$

where $N(t_1)$ is the net FEP count for ^{40}K at 1460.9 keV after the radionuclide diffuses inside the measurement chamber for a period from the starting moment ($t=0$) to t_1 and N_B is the FEP background count for ^{40}K at 1460.9 keV within the measurement time T .

To select a suitable measurement time T , Eq. (15) is used to calculate the measurement accuracies for the FEP background counts at 1460.9 keV on the background γ -spectrometry given by the measurement system within different measurement times.

$$\eta(\%) = \frac{1}{\sqrt{N}} \times 100\%, \tag{15}$$

where η is the measurement accuracy and N is the FEP background counts at 1460.9 keV within the given time. High-accuracy measurements require a value of η less than 5%.

Table S2 lists the calculated η values for the FEP background counts at 1460.9 keV on the background γ -spectrometry given by the measurement system within different measurement times. At $T=65$ min, an η value below 5%, as required for high-accuracy measurements, can be reached. Analysis of the 11 background measurements taken by the measurement system reveals that the mean N_B at 1460.9 keV at $T=65$ min is 417.06, with a mean squared error σ of 8.98. Therefore, when $N(t_1) > 3\sigma$, the confidence level can reach above 99.7% when t_1 is set as the warning time.

The net FEP count for ^{40}K at 1460.9 keV, $N(t_1)$, and the diffusion time of the radionuclide inside the measurement chamber, t_1 , at $T=65$ min can be calculated for the 10 Bq/L ^{40}K radioactive solution using Eqs. (14) and (9), respectively:

$$\begin{cases} N(t_1) = 279.43 \\ t_1 = 3325 \end{cases} \tag{16}$$

Under this condition, the calculated value of $N(t_1)$ is much higher than 3σ . The preset warning threshold allows for effective warning of radioactive contamination in water. In addition, for the 10 Bq/L ^{40}K radioactive solution, the measurement system gives warning 55.42 min after the entry of the radionuclide into the measurement chamber. Subsequently, Eq. (10) is used to calculate the radionuclide activity concentrations in the water at different time intervals between t_1 and t_2 , Δt (as listed in Table S3). When the measurement was continued for an

additional period of 14 min after the warning threshold of the measurement system was reached, the relative deviation of the radionuclide activity concentration provided by the NSS measurement model from the true value was less than 5%.

Based on the above findings, the measurement time T and Δt should be set to 65 and 14 min, respectively, in the NSS measurement model established in this study for the selected online water γ -spectrometry system when used in actual measurement conditions. The following procedure was used to calculate the radionuclide activity concentration in the monitored water: The time at which the warning threshold of the measurement system was reached was defined as t_1 . In addition, the net FEP count for the characteristic γ -rays at t_1 , $N(t_1)$, and that at the time t_2 after 14 min of continual measurements, $N(t_2)$, were recorded. Then, the $N(t_2)/N(t_1)$ ratio, k , was substituted into Eq. (13) to calculate the diffusion time of the radionuclide inside the measurement chamber (i.e., t_1) when the warning threshold of the measurement system was reached at the Δt of 14 min. Finally, substituting the obtained calculation results into Eq. (10) provided an activity concentration estimate for the radionuclides in the monitored water.

Table 4 summarizes the times required by the measurement system to reach the warning threshold at actual measurement conditions ($T=65$ min; $\Delta t=14$ min) for ^{40}K radioactive solutions with different activity concentrations as well as the relative deviations of the estimated activity concentrations of the radionuclide in the water from the true values. The measurements show that the NSS measurement model established in this study is effective in accurately estimating the radionuclide activity concentration in water under actual measurement conditions.

Further analysis of the detection efficiencies of the measurement system for characteristic γ -rays at different energy levels simulated using the Monte Carlo method reveals that their ratios are fixed when they level off. Therefore, the activity concentrations of different radionuclides at the same count rate can be mutually converted based on the emission

Table 4 Warning times and relative deviations of the estimates given by the NSS measurement model from the true values for ^{40}K radioactive solutions with different activity concentrations

True activity concentration (Bq/L)	Warning times (min)	Estimated activity concentration (Bq/L)	Relative error (%)
10	55.42	9.61 ± 0.71	- 3.90
20	34.39	20.31 ± 1.13	1.53
30	27.54	29.46 ± 1.46	- 1.79
40	20.97	39.26 ± 1.85	- 1.85
60	18.33	59.49 ± 2.56	- 0.85
80	15.02	78.63 ± 3.85	- 1.71
100	14.00	99.11 ± 3.87	- 0.89

Table 5 Times required by the measurement system to give warning when the activity concentrations of different radionuclides reach their respective limits stipulated in the Guidelines for Drinking-water Quality (GDWQ) of the World Health Organization

Radionuclide	γ -ray energy (keV)	Guidance level (Bq/L)	Corresponding ^{40}K activity concentration (Bq/L)	Early warning time (min)
^{58}Co	810.71	100	1233.86	15.00 \pm 0.13
^{60}Co	1332.51	100	981.64	15.00 \pm 0.11
^{131}I	364.49	10	139.95	15.01 \pm 0.17
^{134}Cs	604.72	10	138.51	15.01 \pm 0.12
^{137}Cs	661.66	10	115.56	15.05 \pm 0.14

probability and detection efficiency of the measurement system for their characteristic γ -rays at different energy levels. The analysis based on the fitting equation for the variation in the warning time with an activity concentration of ^{40}K in water in Figure S5 shows that the measurement system requires approximately 15 min to provide a warning when the activity concentration of each radionuclide in Table 5 reaches the limit stipulated in the guidelines for drinking-water quality (GDWQ) of the World Health Organization [38].

5 Conclusion

This study presents an NSS measurement model for radionuclide activity concentrations in water to complement online water γ -spectrometry systems designed for inland waters that mostly extract samples in situ and in real time. On this basis, a method is developed to facilitate the online water γ -spectrometry system to give rapid warning and activity estimates in NSS conditions. The experimental results show that when coupled with the NSS measurement model, the measurement system is able to give warning and obtain an accurate estimate for the activity concentration of the radionuclide (^{40}K) in water 55.42 and 69.42 min, respectively, after the entry of a 10 Bq/L ^{40}K radioactive solution (corresponding to a 0.87 Bq/L ^{137}Cs radioactive solution) into the measurement chamber, and the relative error of activity concentration is below $\pm 5\%$. These times are much shorter than the 90 min required for the conventional measurement method. In addition, the NSS method allows the measurement system to provide rapid (within approximately 15 min) warnings when the activity concentrations of some radionuclides reach their respective limits, as stipulated in the GDWQ of the World Health Organization. These results show that the method developed in this study allows online water γ -spectrometry systems to give rapid warning and produce activity estimates in NSS conditions. Therefore, this method significantly improves the timeliness of the monitoring of the radioactivity levels of inland waters that receive effluent from nearby nuclear facilities. It can provide rapid and reliable measurement data to facilitate daily monitoring

of the radioactivity levels of inland waters and monitoring of nuclear emergencies.

Supplementary Information The online version contains supplementary material available at <https://doi.org/10.1007/s41365-024-01395-4>.

Author contributions All authors contributed to the study conception and design. Material preparation, data collection, and analysis were performed by MW, YG, HL, M-LX, and L-QG. The first draft of the manuscript was written by MW, and all authors commented on previous versions of the manuscript. All authors read and approved the final manuscript.

Data availability The data that support the findings of this study are openly available in Science Data Bank at <https://doi.org/10.57760/sciencedb.09014> and <https://cstr.cn/31253.11.sciencedb.09014>.

Declarations

Conflict of interest The authors declare that they have no competing interests.

References

1. M. Aoyama, D. Tsumune, Y. Inomata et al., Mass balance and latest fluxes of radiocesium derived from the Fukushima accident in the western North Pacific Ocean and coastal regions of Japan. *J. Environ. Radioactiv.* **217**, 106206 (2020). <https://doi.org/10.1016/j.jenvrad.2020.106206>
2. K. Buesseler, M.H. Dai, M. Aoyama et al., Fukushima daiichi-derived radionuclides in the ocean: transport, fate, and impacts. *Annu. Rev. Mar. Sci.* **9**, 173–203 (2017). <https://doi.org/10.1146/annurev-marine-010816-060733>
3. K. Buesseler, Fukushima and ocean radioactivity. *Oceanography* **27**, 92–105 (2014). <https://doi.org/10.5670/oceanog.2014.02>
4. H. Kofuji, In situ measurement of ^{134}Cs and ^{137}Cs in seabed using underwater γ -spectrometry systems: application in surveys following the Fukushima Dai-ichi nuclear power plant accident. *J. Radioanal. J. Radioanal. Nucl. Chem.* **303**, 1575–1579 (2015). <https://doi.org/10.1007/s10967-014-3702-0>
5. J.L. Burnett, P.W. Eslinger, B.D. Milbrath, The detectability of the Wigwam underwater nuclear explosion by the radionuclide stations of the international monitoring system. *J. Environ. Radioactiv.* **208–209**, 106030 (2019). <https://doi.org/10.1016/j.jenvrad.2019.106030>
6. D.W. Dou, Z. Zeng, W. Yu et al., In-situ seawater gamma spectrometry with LaBr_3 detector at a nuclear power plant outlet. *J. Mar. Sci. Eng.* **9**, 721 (2021). <https://doi.org/10.3390/jmse9070721>

7. S. Aytas, S. Erenturk, M.A.A. Aslani et al., Determination and evaluation of natural radioactivity and heavy metal levels in the aquatic environment of trans-boundary rivers: Maritza, Tundja and Arda. *J. Radioanal. Nucl. Chem.* **300**, 933–945 (2014). <https://doi.org/10.1007/s10967-014-3091-4>
8. C. Tsabaris, C. Bagatelas, T. Dakladas et al., An autonomous in situ detection system for radioactivity measurements in the marine environment. *Appl. Radiat. Isotopes* **66**, 1419–1426 (2008). <https://doi.org/10.1016/j.apradiso.2008.02.064>
9. F. Ambrosino, L. Stellato, C. Sabbarese, A case study on possible radiological contamination in the Lo Uttaro landfill site (Caserta, Italy). *J. Phys. Conf. Ser.* **1548**, 012001 (2020). <https://doi.org/10.1088/1742-6596/1548/1/012001>
10. Q. Yang, L. Wang, H.Y. Du et al., Investigation of radioactive level of drinking water sources in the Upper Yangtze River of Chongqing city. *J. Radioanal. Nucl. Chem.* **321**, 141–149 (2019). <https://doi.org/10.1007/s10967-019-06551-4>
11. R.Q. Zhang, J.Y. Wang, N.J. Zhao et al., Rapid determination of gross alpha/beta activity in water based on reverse osmosis membrane enrichment pretreatment. *Sci. Technol. Nucl. Install.* **2022**, 2868792 (2022). <https://doi.org/10.1155/2022/2868792>
12. D.G. Jones, Development and application of marine gamma-ray measurements: a review. *J. Environ. Radioactiv.* **53**, 313–333 (2001). [https://doi.org/10.1016/S0265-931X\(00\)00139-9](https://doi.org/10.1016/S0265-931X(00)00139-9)
13. W.H. Lv, Z. Zeng, H.C. Yi et al., Real-time monitoring of gross beta radioactivity in tap water and committed effective dose. *Health Phys.* **115**, 375–381 (2018). <https://doi.org/10.1097/HP.00000000000000896>
14. C. Wedekind, G. Schilling, M. Grüttmüller et al., Gamma-radiation monitoring network at sea. *Appl. Radiat. Isotopes* **50**, 733–741 (1999). [https://doi.org/10.1016/S0969-8043\(98\)00062-1](https://doi.org/10.1016/S0969-8043(98)00062-1)
15. C. Tsabaris, D. Ballas, On line gamma-ray spectrometry at open sea. *Appl. Radiat. Isotopes* **62**, 83–89 (2005). <https://doi.org/10.1016/j.apradiso.2004.06.007>
16. D.S. Vlachos, Self-calibration techniques of underwater gamma ray spectrometers. *J. Environ. Radioactiv.* **82**, 21–32 (2005). <https://doi.org/10.1016/j.jenvrad.2004.11.004>
17. I. Osvath, P.P. Povinec, H.D. Livingston et al., Monitoring of radioactivity in NW Irish Sea water using a stationary underwater gamma-ray spectrometer with satellite data transmission. *J. Radioanal. Nucl. Chem.* **263**, 437–440 (2005). <https://doi.org/10.1007/s10967-005-0073-6>
18. C. Tsabaris, Monitoring natural and artificial radioactivity enhancement in the Aegean Sea using floating measuring systems. *Appl. Radiat. Isotopes* **66**, 1599–1603 (2008). <https://doi.org/10.1016/j.apradiso.2008.01.020>
19. D. Keith, D. Colton, H. Louft et al., New technology for conducting radiation hazard assessments: the application of the underwater radiation spectral identification system (URSIS) at the Massachusetts bay industrial waste (USA). *Environ. Monit. Assess.* **54**, 259–282 (1999). <https://doi.org/10.1023/A:1005998211691>
20. A. Chernyaev, I. Gaponov, A. Kazennov, Direct methods for radionuclides measurement in water environment. *J. Environ. Radioactiv.* **72**, 187–194 (2004). [https://doi.org/10.1016/S0265-931X\(03\)00201-7](https://doi.org/10.1016/S0265-931X(03)00201-7)
21. I. Baranov, I. Kharitonov, L. Andrey et al., Devices and methods used for radiation monitoring of sea water during salvage and transportation of the Kursk nuclear submarine to dock. *Nucl. Instrum. Meth. A* **505**, 439–443 (2003). [https://doi.org/10.1016/S0168-9002\(03\)01116-1](https://doi.org/10.1016/S0168-9002(03)01116-1)
22. P.P. Povinec, I. Osvath, M.S. Baxter, Underwater gamma-spectrometry with HPGe and NaI(Tl) detectors. *Appl. Radiat. Isotopes* **47**, 1127–1133 (1996). [https://doi.org/10.1016/S0969-8043\(96\)00118-2](https://doi.org/10.1016/S0969-8043(96)00118-2)
23. I. Osvath, P.P. Povinec, Seabed γ -ray spectrometry: applications at IAEA-MEL. *J. Environ. Radioactiv.* **53**, 335–349 (2001). [https://doi.org/10.1016/S0265-931X\(00\)00140-5](https://doi.org/10.1016/S0265-931X(00)00140-5)
24. B. Thornton, S. Ohnishi, T. Ura et al., Continuous measurement of radionuclide distribution off Fukushima using a towed sea-bed gamma ray spectrometer. *Deep Sea Res. Part I* **79**, 10–19 (2013). <https://doi.org/10.1016/j.dsr.2013.05.001>
25. R. Casanovas, J.J. Morant, M. Salvadó, Energy and resolution calibration of NaI(Tl) and LaBr₃(Ce) scintillators and validation of an EGS5 Monte Carlo user code for efficiency calculations. *Nucl. Instrum. Meth. A* **675**, 78–83 (2012). <https://doi.org/10.1016/j.nima.2012.02.006>
26. C. Tsabaris, D.L. Patiris, A.P. Karageorgis et al., In-situ radionuclide characterization of a submarine groundwater discharge site at Kalogria Bay, Stoupa, Greece. *J. Environ. Radioactiv.* **108**, 50–59 (2012). <https://doi.org/10.1016/j.jenvrad.2011.08.005>
27. E. Prieto, R. Casanovas, M. Salvadó, Calibration and performance of a real-time gamma-ray spectrometry water monitor using a LaBr₃(Ce) detector. *Radiat. Phys. Chem.* **144**, 444–450 (2018). <https://doi.org/10.1016/j.radphyschem.2017.10.008>
28. X. Guan, L.Q. Ge, G.Q. Zeng et al., Determination of gross α and β activities in Zouma River based on online HPGe gamma measurement system. *Nucl. Sci. Tech.* **31**, 120 (2020). <https://doi.org/10.1007/s41365-020-00828-0>
29. G.Q. Zeng, Z. Zhu, L.Q. Ge et al., Efficiency calibration of HPGe detector used in water γ radioactivity measurement. *Nucl. Tech.* **40**, 120402 (2017). <https://doi.org/10.11889/j.0253-3219.2017.hjs.40.120402>. (in Chinese)
30. Z. Zeng, X.Y. Pan, H. Ma et al., Optimization of an underwater in-situ LaBr₃: Ce spectrometer with energy self-calibration and efficiency calibration. *Appl. Radiat. Isotopes* **121**, 101–108 (2017). <https://doi.org/10.1016/j.apradiso.2016.12.016>
31. Y.Y. Zhang, C.K. Li, D.Y. Liu et al., Monte Carlo simulation of a NaI(Tl) detector for in situ radioactivity measurements in the marine environment. *Appl. Radiat. Isotopes* **98**, 44–48 (2015). <https://doi.org/10.1016/j.apradiso.2015.01.009>
32. J.I. Byun, J.H. Rho, S.W. Choi, A shipboard real-time gamma-ray measurement system for detecting radionuclides in seawater. *Nucl. Instrum. Meth. A* **1005**, 165374 (2021). <https://doi.org/10.1016/j.nima.2021.165374>
33. Y.M. Wang, Y.Y. Zhang, N. Wu et al., Monte Carlo simulation of in situ gamma-spectra recorded by NaI (Tl) detector in the marine environment. *J. Ocean Univ. China* **14**, 471–474 (2015). <https://doi.org/10.1007/s11802-015-2841-4>
34. J.I. Byun, S.W. Choi, M.H. Song et al., A large buoy-based radioactivity monitoring system for gamma-ray emitters in surface seawater. *Appl. Radiat. Isotopes* **162**, 109172 (2020). <https://doi.org/10.1016/j.apradiso.2020.109172>
35. C.H. Dong, K.Y. Liao, R.Y. Xu et al., Design and preliminary test of tritiated water online detector system based on plastic scintillators. *Nucl. Sci. Tech.* **33**, 128 (2022). <https://doi.org/10.1007/s41365-022-01115-w>
36. H. Yang, X.Y. Zhang, W.G. Gu et al., A novel method for gamma spectrum analysis of low-level and intermediate-level radioactive waste. *Nucl. Sci. Tech.* **34**, 87 (2023). <https://doi.org/10.1007/s41365-023-01236-w>
37. H.G. Weller, G. Tabor, H. Jasak et al., A tensorial approach to computational continuum mechanics using object-oriented techniques. *Comput. Phys.* **12**, 620–631 (1998). <https://doi.org/10.1063/1.168744>
38. W.H. Organization. Guidelines for drinking-water quality: Fourth edition incorporating the first addendum. (2017)

Springer Nature or its licensor (e.g. a society or other partner) holds exclusive rights to this article under a publishing agreement with the author(s) or other rightsholder(s); author self-archiving of the accepted manuscript version of this article is solely governed by the terms of such publishing agreement and applicable law.